Available online at www.sciencedirect.com

ScienceDirect

Journal of Power Sources 180 (2008) 322–329

JOURNAL OF POWER SOURCES

www.elsevier.com/locate/jpowsour

Model predictive control of water management in PEMFC

Liyan Zhang [a,b,*], Mu Pan [a], Shuhai Quan [b]

[a] *State Key Laboratory of Advanced Technology for Materials Synthesis and Progressing, Wuhan University of Technology, Wuhan 430070, China*

[b] *School of Automation, Wuhan University of Technology, Wuhan 430070, China*

Received 11 December 2007; received in revised form 25 January 2008; accepted 28 January 2008

Available online 16 February 2008

Abstract

Water management is critical for Proton Exchange Membrane Fuel Cells (PEMFC). An appropriate humidity condition not only can improve the performances and efficiency of the fuel cell, but can also prevent irreversible degradation of internal composition such as the catalyst or the membrane. In this paper we built the model of water management systems which consist of stack voltage model, water balance equation in anode and cathode, and water transport process in membrane. Based on this model, model predictive control mechanism was proposed by utilizing Recurrent Neural Network (RNN) optimization. The models and model predictive controller have been implemented in the MATLAB and SIMULINK environment. Simulation results showed that this approach can avoid fluctuation of water concentration in cathode and can extend the lifetime of PEM fuel cell stack.

Keywords: Proton Exchange Membrane Fuel Cell (PEMFC); Water management; Model predictive control (MPC); Recurrent neural network (RNN)

1. Introduction

Proton Exchange Membrane Fuel Cells (PEMFC) (also known as Polymer Electrolyte Membrane Fuel Cells) is currently in a relatively mature stage for ground vehicle applications. For PEMFC the membrane must be sufficiently hydrated because its conductivity depends critically on the humidity level. Too little water causes membrane drying, which increases the ionic resistance, and exacerbates the voltage drop due to ohmic losses. Too much water causes “flooding”, which blocks porous passages and thus reduces the transport rate of reactants to the catalyst site [1]. An inappropriate humidity condition not only can lower the performances and efficiency of the fuel cell but also can even lead to an irreversible degradation of internal component such as the catalysts or the membrane. For examples, these will lead to catalysts desquamated and membrane damaged in the alternate wet and dry condition. Therefore, water management is a critical issue for PEMFC.

There were many papers in the literature discussing the fuel cell water management issues. Many experimental studies were conducted to understand the water transport phenomena and to characterize the factors that affect the membrane water content [2,3]. Shimpalee et al. [4] studied a time dependence of three-dimensional simulation including water phase change and heat transfer of a PEMFC model. The overshoot behavior has been observed during a change in the electrical load during operation with fixed flow rates of hydrogen and air. Some mathematic models have been developed to optimize the fuel cell design in order to maintain appropriate membrane humidity of PEMFC stack. Chen et al. [5] built a one-dimension model to investigate the transient behavior of the water transport across the membrane of the PEMFC. Alessandro et al. [6] developed a control-oriented model of the fuel cell system based on static maps obtained from a higher order 1&1D model. Wolfgang et al. [7] set up a test bench to measure the ohmic resistance of fuel cell stack and showed that the humidity of membrane has a very strong influence on the electrical output of a fuel cell. Gorgun et al. [1,8] presented a scheme to estimate membrane water content in PEMFC from the measurements of voltage, current, temperature and reactant pressure. Hung et al. [9] developed a first principle one-dimensional water and thermal management model to generate the *I–V* curve. The model considers the effects of water

* Corresponding author at: State Key Laboratory of Advanced Technology for Materials Synthesis and Progressing, Wuhan University of Technology, Wuhan 430070, China. Tel.: +86 27 62767750; fax: +86 27 87866049.

E-mail address: zeroplus@tom.com (L. Zhang).

0378-7753/$ – see front matter © 2008 Elsevier B.V. All rights reserved.
doi:10.1016/j.jpowsour.2008.01.088

Nomenclature

a	water activity
A_{fc}	fuel cell active area (cm^2)
c	water concentration (mol cm^{-3})
D_w	diffusion coefficient
E_0	the open circuit voltage
F	Faraday's number (C)
I	stack current (A)
J	rotational inertia (kg m^2)
m	mass (kg)
M	molecular mass (kg mol^{-1})
n	number of cells
n_d	The electro-osmotic drag coefficient
P	pressure (Pa)
R	gas constant
R'	electrical resistance (Ω)
T	temperature (K)
V	voltage (V)
V'	volume (cm^3)
W	mass flow rate (kg s^{-1})
t	time (s)
t_m	membrane thickness (cm)
x	volume content of dry air
y	mole fraction of dry air

Greek letters

Ω	humidity ratio
ϕ	relative humidity
λ_m	membrane average water content
σ_m	the membrane conductivity

Subscripts

act	activation
a, air	air
atm	atmosphere
H_2	hydrogen
an	anode
ca	cathode
conc	concentration
fc	fuel cell
gen	generated
in	inlet
inj	inject
m, mbr	membrane
N_2	nitrogen
O_2	oxygen
ohm	ohmic
out	outlet
rct	reaction
rm	return manifold
sat	saturation
sm	supply manifold
st	stack
v	vapor
w	water

transport across the membrane, activation overpotential, ohmic overpotential, concentration overpotential, pressure drops, and current density distribution along the channel of a PEM fuel cell.

Although many researchers studied the mechanism of water management and built 3D, 2D, 1D or 0D model, few researchers explored how to control the humidity of PEMFC stack. Trung and Knobbe [10] presented an excess water removal method by controlling each cell's exhaust so that only one cell at any given time has an open exhaust port, thereby, ensuring gas will flow through that cell. Chen and Peng [11] built model of humidifier system and developed proportional feedback control algorithm to regulate the inlet air relative humidity. A fuzzy controller is proposed for water management of PEM based on Mamadani inference systems [12]. In this paper, we built model of water management system and proposed model predictive control to maintain appropriate humidity of membrane in PEMFC. Model Predictive Control (MPC) is widely adopted in industry as an effective means to deal with large multivariable constrained control problems. In general, the MPC problem is formulated as solving on-line a finite horizon open-loop optimal control problem subject to system dynamics and constraints involving state and control variables. There are some literatures discussing MPC methods of PEMFC. Golbert [13] developed MPC controller based on the simplified nonlinear model which satisfies load-change demands and improves fuel efficiency. Vahidi et al. [14] proposed constraint MPC to prevent oxygen starvation in a fuel cell during rapid current transients.

2. Model of water management system

In PEMFC stack oxygen and hydrogen are consumed, and water and heat are generated. Generally, a PEMFC stack is integrated with four auxiliary systems: hydrogen supply system, air supply system, cooling system and humidification system. Water management system, which is humidification system, is used to maintain hydration of the polymer membrane and to balance water consumption in the system. The amount of reactant flow and the water injected into the anode and cathode flow streams affect the humidity of the membrane. Dry membranes and flooded fuel cells cause high polarization losses. As the current is drawn from the fuel cell, water molecules are produced in the cathode and dragged from the anode to the cathode by the hydrogen protons. As the concentration of water in the cathode increases, the concentration gradient causes water to diffuse from the cathode to the anode. Perturbation in fuel cell humidity can be caused by different mechanisms: water generated while load increases, changes in the absolute and relative reactant pressure across the membrane, changes in air flow rate and changes in stack temperature, which change the vapor saturation pressure [15]. These mechanisms indicate strong and nonlinear interaction among the humidity control tasks. A 20–40% drop in voltage can occur if there is no proper humidification control [16].

We build water balance equation by investigating stack voltage model, water distribution of membrane and water transport process in cathode and anode. In this paper direct injection of water into cathode is used for humidification. The following equations are stack voltage model, water distribution of membrane and water balance equation of cathode and anode.

2.1. Water balance equation in anode

The governing equation for hydrogen and water in the anode can be written as

$$\mathrm{d}m_{H_2}/\mathrm{d}t = W_{H_2,in} - W_{H_2,out} - W_{H_2,rct} \quad (1)$$

$$\mathrm{d}m_{w,an}/\mathrm{d}t = W_{v,an,in} - W_{v,an,out} - W_{v,mbr} \quad (2)$$

The hydrogen and water flowing to the anode are calculated by

$$W_{H_2,in} = (1 - \Omega_{an,in})W_{an,in} \quad (3)$$

$$W_{v,an,in} = \Omega_{an,in} W_{an,in} \quad (4)$$

where $\Omega_{an,in}$ is inlet flow humidity ratio in anode.

The outlet hydrogen and vapor mass flow rate is calculated by the following equations.

$$W_{H_2,an,out} = 1/(1 + \Omega_{an,out})W_{an,out} \quad (5)$$

$$W_{v,an,out} = \phi_{an,out}/(1 + \Omega_{an,out})W_{an,out} \quad (6)$$

$$\Omega_{an,out} = M_v/M_{H_2} \cdot (m_{H_2} R_{H_2})/(m_{v,an} R_{H_2}) \quad (7)$$

The rate of water flow across the membrane $W_{v,mbr}$ is determined in the membrane hydrogen model. The rate of hydrogen consumed in the reaction $W_{H_2,rct}$ is a function of the stack current

$$W_{H_2,rct} = M_{H_2}(nI_{st})/(2F) \quad (8)$$

2.2. Water balance equation in cathode

The mass continuity is used to balance the mass of the three elements: oxygen, nitrogen and water, inside the cathode volume [17].

$$\mathrm{d}m_{O_2}/\mathrm{d}t = W_{O_2,in} - W_{O_2,out} - W_{O_2,rct} \quad (9)$$

$$\mathrm{d}m_{N_2}/\mathrm{d}t = W_{N_2,in} - W_{N_2,out} \quad (10)$$

$$\mathrm{d}m_{w,ca}/\mathrm{d}t = W_{v,ca,in} - W_{v,ca,out} + W_{v,gen} + W_{v,mbr} + W_{inj} \quad (11)$$

where W_{inj} is the mass flow rate of injected water from humidifier. Inlet mass of oxygen, nitrogen and vapor is related to mass flow rate and humidity of inlet air.

$$W_{O_2,in} = y_{O_2}/(1 + \Omega_{atm})W_{ca,in} \quad (12)$$

$$W_{N_2,in} = y_{N_2}/(1 + \Omega_{atm})W_{ca,in} \quad (13)$$

$$W_{v,ca,in} = \Omega_{atm}/(1 + \Omega_{atm})W_{ca,in} \quad (14)$$

y_{O_2} and y_{N_2} are oxygen mole fraction and nitrogen mole fraction of dry air.

$$y_{O_2} = x_{O_2} \cdot M_{O_2}/M_a^{atm} \quad (15)$$

$$y_{N_2} = (1 - x_{O_2}) \cdot M_{N_2}/M_a^{atm} \quad (16)$$

where x_{O_2} is volume content of oxygen in dry air. The air molar mass is calculated by

$$M_a^{atm} = x_{O_2} M_{O_2} + (1 - x_{O_2})M_{N_2} \quad (17)$$

The humidity ratio is then

$$\Omega_{atm} = M_v/M_a \cdot \phi_{atm} P_{sat}^{atm}/(P_{atm} - \phi_{atm} P_{sat}^{atm}) \quad (18)$$

The pressure of cathode is the sum of the partial pressure of oxygen, nitrogen and vapor.

$$p_{ca} = p_{O_2} + p_{N_2} + p_{v,ca} \quad (19)$$

According to ideal gas law, the partial pressure of oxygen, nitrogen and vapor is

$$p_{O_2} = (m_{O_2} R_{O_2} T_{st})/V'_{ca} \quad (20)$$

$$p_{N_2} = (m_{N_2} R_{N_2} T_{st})/V'_{ca} \quad (21)$$

$$p_{v,ca} = (m_{v,ca} R_v T_{st})/V'_{ca} \quad (22)$$

Outlet gas flow rate is calculated by [15]

$$W_{ca,out} = k_{ca,out}(P_{ca} - P_{rm,ca}) \quad (23)$$

where the mass flow rate of each species out of the cathode is calculated as

$$W_{O_2,out} = W_{ca} \cdot m_{O_2}/m_{ca} \quad (24)$$

$$W_{N_2,out} = W_{ca} \cdot m_{N_2}/m_{ca} \quad (25)$$

$$W_{v,ca,out} = (p_{v,ca} V'_{ca} M_v)/(RT_{st} m_{ca}) \cdot W_{ca} \quad (26)$$

where $m_{ca} = m_{O_2} + m_{N_2} + (p_{v,ca} V_{ca} M_v)/(RT_{st})$ is the total mass of the cathode gas.

The rate of hydrogen consumed in the reaction and water generated in the reaction is calculated by

$$W_{O_2,rct} = M_{O_2}(nI_{st})/(4F) \quad (27)$$

$$W_{v,gen} = M_{H_2O}(nI_{st})/(2F) \quad (28)$$

2.3. Water transport process in membrane

The water transport across the membrane is achieved through two distinct phenomena [18]. First, water molecules are dragged across the membrane from anode to cathode by the hydrogen proton. This phenomenon is called electro-osmotic. Secondly, the gradient of water concentration across the membrane results in “back-diffusion” of water, usually from cathode to anode. The water concentration is assumed to change linearly over the membrane thickness. Combining the two water transport mechanisms, the water flow across the membrane from anode to cathode [15] is

$$W_{v,mem}=M_v A_{fc} n(n_d I_{st}/F - D_w \cdot (c_{v,an} - c_{v,an})/t_m) \quad (29)$$

The electro-osmotic drag coefficient n_d and the diffusion coefficient D_w vary with water content in the membrane [19,20].

$$n_d = 0.0029\lambda_m^2 + 0.05\lambda_m - 3.4 \times 10^{-19} \quad (30)$$

$$D_w = D_\lambda \exp(2416(1/303 - 1/T_{st})) \quad (31)$$

where

$$D_\lambda = \begin{cases} 10^{-6}, & \lambda_m < 2 \\ 10^{-6}(1 + 2(\lambda_m - 2)), & 2 \le \lambda_m \le 3 \\ 10^{-6}(3 - 1.67(\lambda_m - 3)), & 3 < \lambda_m < 4.5 \\ 1.25 \times 10^{-6}, & \lambda_m \ge 4.5 \end{cases} \quad (32)$$

Membrane average water content λ_m is calculated by [19,20]

$$\lambda_m = \begin{cases} 0.043 + 17.81a_m - 39.85a_m^2 + 36.0a_m^3, & 0 < a_m \le 1 \\ 14 + 1.4(a_m - 1), & 1 < a_m \le 3 \end{cases} \quad (33)$$

where

$$a_m = (a_{an} + a_{ca})/2 \quad (34)$$

Water activities in anode and cathode a_{an} and a_{ca} is calculated by

$$a_{an} = P_{v,an}/P_{sat,an}, \quad a_{ca} = P_{v,ca}/P_{sat,ca} \quad (35)$$

2.4. Stack voltage model

The stack voltage is calculated as a function of stack current, cathode pressure, reactant partial pressures, stack temperature and membrane humidity. There are a lot of stack voltage model in the literature. We adopt the semi-empirical model in this paper [21].

$$V'_{fc} = E_0 - V'_{act} - V'_{ohm} - V'_{conc} \quad (36)$$

where E_0 is the open circuit voltage, V_{act} is the activation voltage loss resulted from the need to move electrons and to break and form chemical bonds in the anode and cathode, V_{ohm} is the ohmic voltage loss resulted from the resistance of the polymer membrane to the protons transfer and the resistance of the electrode and the collector plate to the electrons transfer, V_{conc} is the concentration voltage loss resulted from the drop in concentration of the reactants as they are consumed in the reaction.

E_0 is the function of stack temperature T, pressure of hydrogen P_{H_2} and pressure of oxygen P_{O_2} [15,21]

$$E_0 = 1.229 - 0.85 \times 10^{-3}(T - 298.15) + 4.3085 \times 10^{-5} T \left[\ln(p_{H_2}) + 0.5\ln(p_{O_2})\right] \quad (37)$$

where

$$p_{H_2} = \frac{(m_{H_2} R_{H_2} T_{st})}{V_{an}} \quad (38)$$

Activation voltage loss V_{act} is calculated as follows

$$V_{act} = V_0 + V_a(1 - e^{-c_1 i}) \quad (39)$$

where c_1 is parameter [15,21], V_0 and V_a can be calculated as follows

$$V_0 = 0.279 - 8.5 \times 10^{-4}(T - 298.15) + 4.308 \times 10^{-5} T \cdot \times \left[\ln\left(\frac{p_{ca} - p_{sat}}{1.01325}\right) + \frac{1}{2}\ln\left(\frac{0.01173(p_{ca} - p_{sat})}{1.01325}\right)\right] \quad (40)$$

$$V_a = (-1.618 \times 10^{-5} T + 1.618 \times 10^{-2})\left(\frac{p_{O_2}}{0.1173 + p_{sat}}\right)^2 \times (1.8 \times 10^{-4} T - 0.166)\left(\frac{p_{O_2}}{0.1173 + p_{sat}}\right) + (-5.8 \times 10^{-4} T + 0.5736) \quad (41)$$

Ohmic voltage loss V_{ohm} is calculated as follows

$$V_{ohm} = R' i \cdot_{ohm} = \frac{t_m}{\sigma_m} \quad (42)$$

where t_m is the thickness of membrane, σ_m is the membrane conductivity and calculated as follows

$$\sigma_m = b_1 \exp\left(b_2\left(\frac{1}{303} - \frac{1}{T}\right)\right) \quad (43)$$

in which b_2 is constant [21], b_1 is function of water content of membrane λ_m

$$b_1 = 0.005139\lambda_m - 0.00326 \quad (44)$$

Concentration voltage loss V_{conc} is calculated as follows

$$V_{conc} = i(c_2 i / i_{max})^{c_3} \quad (45)$$

where c_2, c_3 and i_{max} are constant [21].

3. MPC based on RNN

MPC is widely adopted in industry as an effective means to deal with large multivariable constrained control problems. At each sample instance MPC problem has a quadratic objective function and subject to system dynamics and constraints involving state and control variables. So these form the Quadratic programming (QP) problem at each sample instance. As the QP optimization problem depends on the current state, the implementation of MPC requires the online solution of a QP at each sample instance. High computational burden in solving QP problem is a major obstacle when we apply MPC to industrial process. To solve this problem, a novel MPC based on RNN is proposed.

3.1. Formulation of MPC

Consider the following receding horizon formulation:

$$\begin{aligned} \min_u = & \sum_{k=1}^{N} (y(t+k) - y_r)^T Q (y(t+k) - y_r) \\ & + (u(t+k) - u_r)^T R (u(t+k) - u_r) \\ \text{s.t.} \quad & x(t+k+1) = Ax(t+k) + Bu(t+k) \\ & y(t+k+1) = Cx(t+k) + Du(t+k) \\ & u_{min} \le u(t+k) \le u_{max} \end{aligned} \quad (46)$$

where $x(t+k) \in R^n$ is the expected value of the state variable at the time $t+k$ as predicted at the time t, $y(t+k) \in R^p$ is the corresponding output variable, $u(t+k) \in R^m$ is manipulated variables considered in the optimization program at the time $t+k$ as predicted at the time t. N is predictive horizon, y_r and u_r are reference trajectory of output variable and manipulated variable, respectively. $Q\in R^{p\times p}$ and $R\in R^{m\times m}$ are weight matrices. $x(t+k+1)=Ax(t+k)+Bu(t+k)$ and $y(t+k+1)=Cx(t+k)+Du(t+k)$ are plant model.

It is well known that MPC solves this problem at each sample instance t by computing all next N values of the manipulated variables $u(t+k)$. According to system model, we can get

$$x(t+k+1)=A^k x(t)+\sum_{i=1}^{k}A^{k-i}Bu(t+i) \quad y(t+k+1) = CA^{k-1}x(t)+\sum_{i=1}^{k-1}CA^{k-i-1}Bu(t+i)+Du(N) \tag{47}$$

Substituting Eq. (47) into optimization problem (46), we have the form of a QP problem

$$\min_U \left\{\frac{1}{2}U^T HU+(x(t)^T S+T)U\right\} \quad \text{s.t.} \quad U_{\min}\le EU\le U_{\max} \tag{48}$$

where $x(t)$ is value of state variable at time t, $U=[u(t),u(t+1), \ldots ,u(t+N)]^T$ is manipulated variable set in next N step, $H\in R^{mN\times mN}$, $S\in R^{n\times mN}$, $T\in R^{mN}$, $E\in R^{mN\times mN}$ is fixed value matrix and can be easily obtained from the plant and Q, R (for details, see [22]).

3.2. RNN optimization

At each step $x(t)$ is already known in QP problem (48), so we apply RNN proposed by Xia et al. [23] to solve this QP problem.

Consider the Lagrangian function of problem (48)

$$L(x,y,\eta)=\frac{1}{2}x^T Hx+((x(t)^T S+T)U-\lambda^T(EU-\eta)$$

where $\lambda\in R^{mN}$ is referred to as the Lagrange multiplier and $\eta\in X=\{\lambda\in R^{mN}|u_{\min}\le\lambda\le u_{\min}\}$. According to Saddle point theorem, we assume that the value of λ and η are λ^* and η^* when x^* is an optimal solution of the problem (48).

In [23], an approach to transform QP problem into RNN optimization, whose dynamic equation is defined as follows.

State equation

$$\frac{dv}{dt}=\lambda\{P_x(Wu+q-u)-Wu-q\} \tag{49}$$

Output equation

$$U(t)=Rv(t)+a \tag{50}$$

where $W=R=Q^{-1}$ is matrix, $q=a=Q^{-1}(x(1)^T R-T)$ is vector, $v\in R^{mN}$ is the state variable of RNN, $\lambda>0$ is a scaling constant.

$P_X(v)=[P_X(v_1), P_X(v_2), \ldots, P_X(v_{mN})]^T$ and for $i=1,\ldots,m*N$

$$P_X(v_i)=\begin{cases} u_{\min}(i) & v_i<u_{\min}(i)\\ v_i & v_i<u_{\max}(i)\\ u_{\max}(i) & v_i>u_{\max}(i)\end{cases} \tag{51}$$

It can be seen that the state equation described by Eq. (49) can be implemented by an analog circuit with a single-layer structure. The proposed MPC based on RNN method can be summarized as in the following:

(1) Initialization. Let $k=1$. Set terminal time T_{end}, the value of state variable $x(k)$ in plant model, predictive horizon N, control horizon N_c, sample time t, weight matrix Q and P, computation time Δt of RNN at each sample time. According to the plant model, calculate matrix H, S, T and $W=R=H^{-1}$.
(2) Calculate RNN parameters. Calculate $f=S\cdot x(k)+T$, $q=a=-H^{-1}f$.
(3) RNN dynamic optimization. According to W, R, q and a, RNN start to run, after time Δt, we get stable value U^*.
(4) Prediction of plant model. Get first m value in U^* as the value of manipulated variable and calculation next step value $x(t+1)$ of state variable.
(5) If $k<T_{\text{end}}$, set $k=k+1$, return step 2, otherwise, program end.

To study optimization capability of the proposed MPC based on RNN, convergence property of RNN at each sample instance must be investigated. According to theorem in [23], our main result on the proposed MPC based on RNN is the following.

Theorem 1. *The state trajectory of the proposed recurrent neural network is exponentially convergent to a solution of Problem* (48).

Theorem 2. *Assume that $W=EQ^{-1}E^T$ and $q=EQ^{-1}(x(t+1)^T R-T)$, the output trajectory of the proposed RNN converges globally to a unique optimal solution of Problem* (48) *at each step within a finite time. Moreover, it has the following converge rate*

$$||x(t)-x^*||^2\le\frac{\gamma}{\lambda(t-t_0)}, \forall t>t_0$$

where γ is a positive constant.

4. Discussion and results

MPC based on RNN methods are used to improve water management in PEMFC. The control objective of water management is to keep water concentration of cathode in a fixed value and avoid fluctuation of water concentration in cathode.

According to the nonlinear model described in Section 2, the state equations involve five state variables $x=[m_{H_2}, m_{w,an}, m_{O_2}, m_{N_2}, m_{w,ca}]^T$. The parameters used in this model are given in Table 1. Most of the parameters are based on the 75 kW stacks used in the FORD P2000 fuel cell prototype vehicle [15,24]. This stack consists of 381 single fuel cells, the membrane of single fuel cell is Nafion 117. All nonlinear models are implemented in Matlab/Simulink environment. The Simulink block is shown in Fig. 1. This model is capable of capturing the effects of transient humidity on the fuel cell voltage. Even the model has not been validated with an actual experi-

Table 1
Parameter used in the model

Symbol	Variable	Value
M_{H_2}	Hydrogen molar mass	2.016×10^{-3} kg mol^{-1}
M_{O_2}	Oxygen molar mass	32×10^{-3} kg mol^{-1}
M_{N_2}	Nitrogen molar mass	28×10^{-3} kg mol^{-1}
R_{H_2}	Hydrogen gas constant	4124.3 J (kg K)$^{-1}$
R_{N_2}	Nitrogen gas constant	296.8 J (kg K)$^{-1}$
R_{O_2}	Oxygen gas constant	259.8 J (kg K)$^{-1}$
R_v	Vapor gas constant	461.5 J (kg K)$^{-1}$
R_a	Air gas constant	286.9 J (kg K)$^{-1}$
P_{atm}	Atmospheric pressure	101.325 kPa
n	Number of cells in fuel cell stack	381
A_{fc}	Fuel cell active area	280 cm^2
V_{an}	Anode volume	0.005 m^3
V_{ca}	Cathode volume	0.01 m^3
F	Faraday number	96485
$\Omega_{an,in}$	Humidity ratio of hydrogen	0
ϕ_{atm}	Relative humidity of air	0.5

mental system, the model predicts transient behavior similar to that reported in the literature [15].

Firstly, we see the simulation result when we do not control mass flow rate of injected water from humidifier W_{inj}. During 0–3 s time period stack current is 200 A and steps up to 300 A during 3–6 s time period. Mass flow rate of injected water is 0.06 kg s^{-1} during 0–6 s time period. Simulation result is shown in Fig. 2. From Fig. 2 we see that water mass in cathode is about 0.0021 kg during 0–3 s time period and drop to 0.00186 kg during 3–6 s time period, stack voltage is about 264 V during 0–3 s time period and about 208 V during 3–6 s time period. We assumed that the inlet airflow rate is well controlled in all cases. The inlet airflow rate is 0.4 kg s^{-1} during 0–3 s time period and 0.6 kg s^{-1} during 3–6 s time period. If we do not control mass flow rate of injected water when stack current step up from 200 to 300 A, water humidity in cathode cannot maintain a stable value and stack voltage decreased with a large amount.

According to the nonlinear model shown in Fig. 1, we adopt PID controller to control water mass in cathode. Control vari-

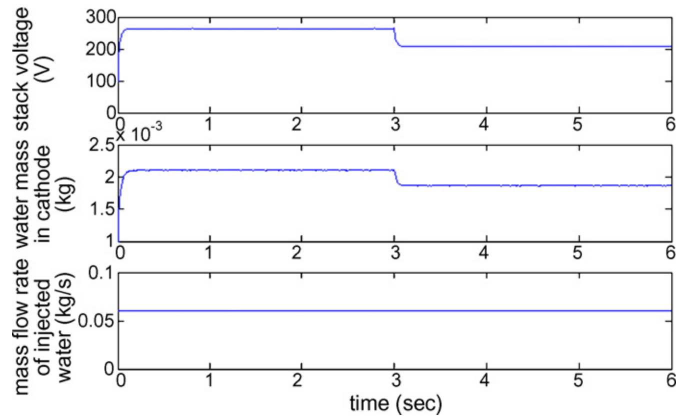

Fig. 2. Simulation result without control.

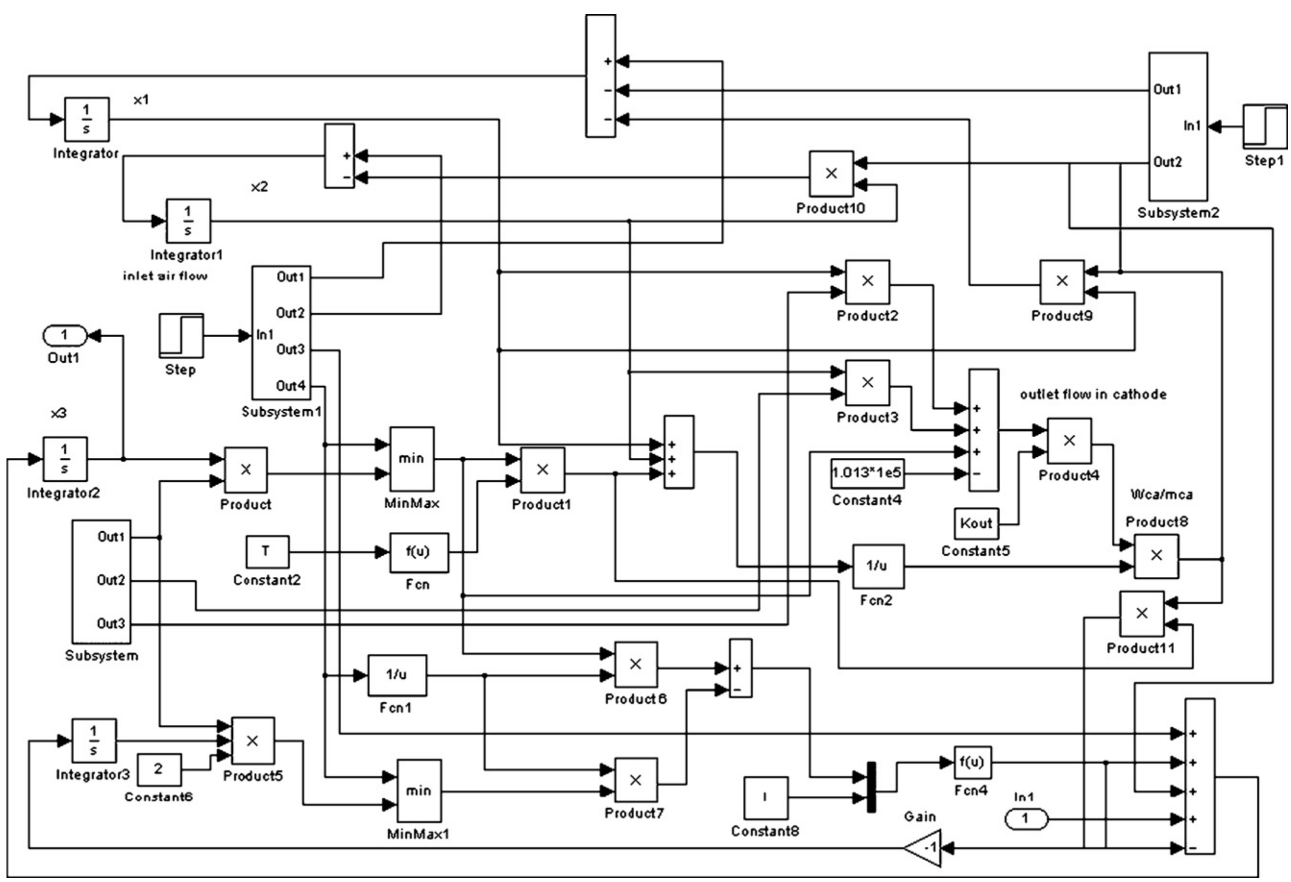

Fig. 1. Simulink block of water management model.

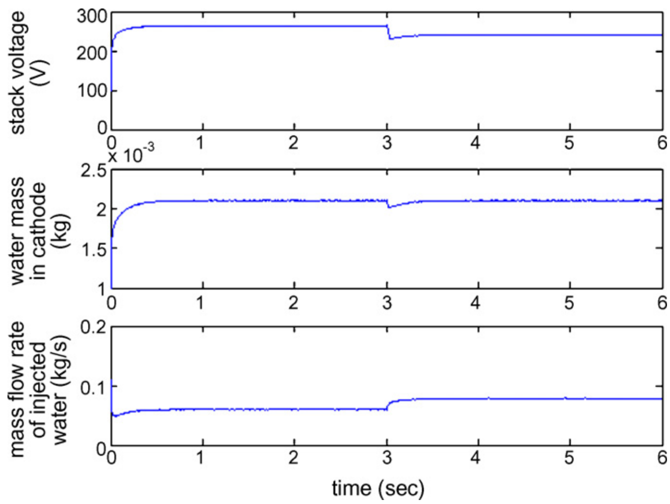

Fig. 3. Simulation result of PID controller.

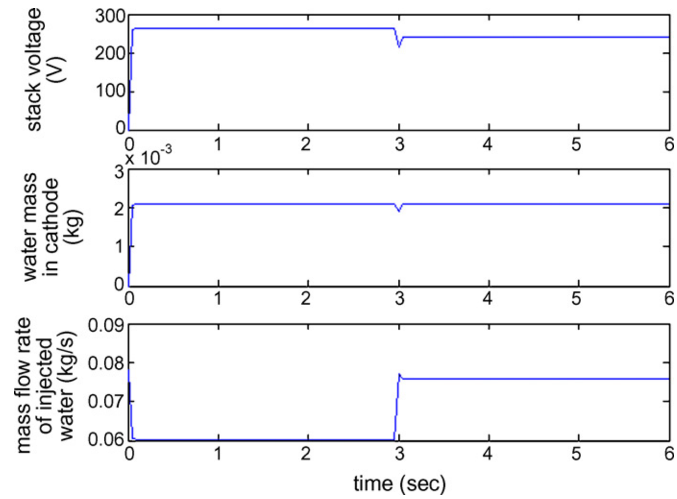

Fig. 5. Simulation result of MPC.

able is mass flow rate of injected water from humidifier W_{inj}. Because it is hard to measure water mass in cathode, we designed an observer of water mass in cathode according to water management model similar as [25]. During 0–3 s time period stack current is 200 A and steps up to 300 A during 3–6 s time period. Simulation result is shown in Fig. 3. We notice that water mass in cathode can be kept at a stable level about 0.0021 kg, stack voltage is about 264 V during 0–3 s time period and about 240.5 V during 3–6 s time period, and the response time is about 0.5 s when stack current steps up.

When we linearize this system at the nominal operating point with stack current as 200 A and stack temperature as 338 K, we can get state space equation $\begin{array}{ll}\dot{x} & = Ax + Bu \\ y & = Cx + Du\end{array}$, where $x = [m_{\mathrm{H_2}}, m_{\mathrm{w,an}}, m_{\mathrm{O_2}}, m_{\mathrm{N_2}}, m_{\mathrm{w,ca}}]^T$, y is the water mass in cathode and u is the flow rate of injected water from humidifier. The reference output is $Y_{\mathrm{r}} = 0.0021$ kg, $P = 1$, $Q = 10$, predictive horizon $N = 3$, sample time $t = 0.1$ s. We used model predictive control based on RNN. In this controller control variable is the flow rate of injected water in humidifier and output variable is water mass in cathode. The RNN has 3 state variables. Transient behaviors of RNN state at each sample instance is shown in Fig. 4. From Fig. 4 we see that x is the state variable of RNN at each sample instance and convergence time is about 0.005 s and 20 times shorter than sample time. So the computation time of RNN optimization is enough to solve the MPC problem at each sample time. Simulation result of MPC controller is shown in Fig. 5. From Fig. 5 we see that water mass in cathode can keep the fixed value about 0.0021 kg, stack voltage is about 264 V during 0–3 s time period and about 240.5 V during 3–6 s time period, and the response time is about 0.15 s when stack current steps up. When the water mass in cathode is 0.0021 kg, humidity in cathode is about 90–100%. Moreover, we simulate continuous change of the multiple stack currents. During 0–3 s time period stack current is 100 A, steps up to 150 A during 3–6 s time period, steps up to 200 A during 6–9 s time period, steps down to 150 A during 9–12 s time period, steps up to 250 A during 12–15 s time period and steps up to 300 A during 15–18 s time period. Simulation result is shown in Fig. 6. So MPC controller can keep humidity of cathode in fixed value. Moreover, MPC controller has shorter response time than PID controller. From

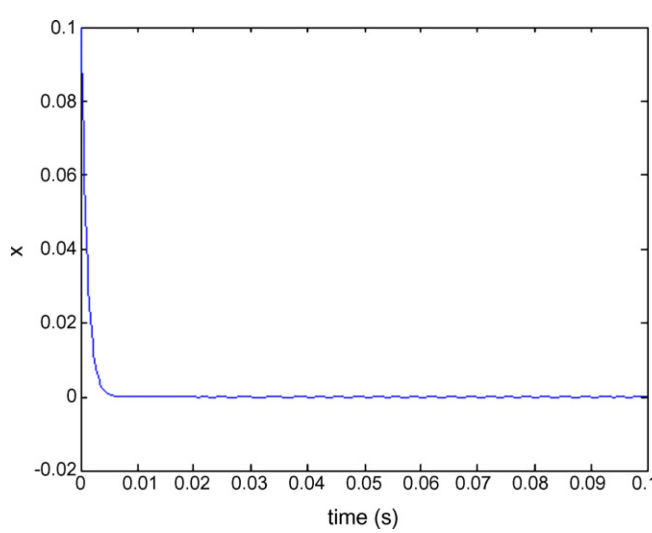

Fig. 4. Transient behaviors of RNN state at each sample instance.

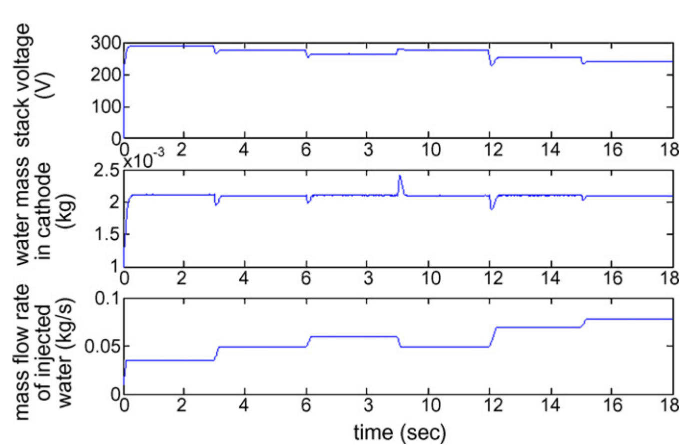

Fig. 6. Simulation result of MPC in different stack current.

the comparisons of three cases: without control, PID control and MPC we can conclude that MPC controller can avoid fluctuation of humidity in cathode and prevent irreversible degradation of internal component such as the catalyst or the membrane.

5. Conclusion

In this paper a detailed model of water management in PEM fuel cell is built and its simulation is implemented in the Matlab/Simulink environment. Based on these model and simulation, we proposed MPC approach to control water concentration in cathode and reduce fluctuation of humidity of cathode. MPC optimization at each sample instance is achieved using RNN optimization. Simulation results showed that MPC controller based on RNN has shorter response time than PID controller and can avoid fluctuation of water concentration in cathode. So this method can be applied to real-time control in water management of PEMFC.

Acknowledgements

This work is funded by the Hi-tech Research and Development Program of China under contract 2006A11A133 and National Natural Science Foundation of China under contract 60705032.

References

[1] H. Gorgun, M. Arcak, F. Barbir, Am. Control Conf. (2005) 4796–4801.
[2] D. Chu, R.Z. Jiang, J. Power Sources 83 (1–2) (1999) 128–133.
[3] O. Tatsuhiro, J. Electroanal. Chem. 465 (1999) 1–17.
[4] S. Shimpalee, D. Spuckler, J.W. Van Zee, J. Power Sources 167 (1) (2007) 130–138.
[5] F.L. Chen, H.S. Chu, C.Y. Soong, W.M. Yan, J. Power Sources 140 (2) (2005) 243–249.
[6] M. Alessandro, D.D. Alfonso, Y.G. Guezennec, S. Rajagopalan, IEEE Vehicle Power Propulsion Conf. (2005) 611–618.
[7] F. Wolfgang, R. Stephane, D. Bernard, IEEE Trans. Power Electrons 19 (5) (2004) 1234–1241.
[8] H. Gorgun, M. Arcak, F. Barbir, J. Power Sources 157 (1) (2006) 389–394.
[9] A.J. Hung, L.Y. Sung, Y.H. Chen, C.C. Yu, J. Power Sources 171 (2) (2007) 728–737.
[10] V.N. Trung, M.W. Knobbe, J. Power Sources 114 (1) (2003) 70–79.
[11] D.M. Chen, H. Peng, Proc. 2004 Am. Control Conf. (2004) 822–827.
[12] H. Abtahi, A. Zilouchian, A. Saenqrung, in: IEEE International Conference on Systems, Man and Cybernetics (2005) 3486–3490.
[13] J. Golbert, D.R. Lewin, J. Power Sources 135 (1–2) (2004) 135–151.
[14] A. Vahidi, A. Stefanpoulou, H. Peng, Proc. Am. Control Conf. (2004) 834–839.
[15] J.T. Pukrushpan, A.G. Stefanopoulou, H. Peng, Control of Fuel Cell Power Systems: Principles, Model, Analysis and Feedback Design, Springer-Verlag, London, 2004, pp. 31–53.
[16] F. Buchi, S. Srinivasan, J. Electrochem. Soc. 144 (8) (1997) 2767–2772.
[17] J.T. Paukrushpan, A.G. Stefanopoulou, H. Peng, IEEE Control Syst. Mag. 24 (2) (2004) 30–46.
[18] T. Nguyen, R. White, J. Electrochem. Soc. 140 (8) (1993) 2178–2186.
[19] S. Shimpalee, S. Dutta, J.W. Van Zee, Proc. ASME IMECE (2000) 1–12.
[20] S. Shimpalee, S. Dutta, Numer. Heat Transfer Part A 38 (2000) 111–128.
[21] J. Amphlett, R. Baumert, R. Mann, B. Peppley, Roberge, J. Electrochem. Soc. 142 (1) (1995) 9–15.
[22] A. Bemporad, M. Morari, V. Dua, E.N. Pistikopoulos, Automatica 38 (2002) 3–20.
[23] Y. Xia, G. Feng, J. Wang, Neural Netw. 17 (7) (2004) 1003–1015.
[24] J.A. Adams, W.C. Yang, K.A. Oglesby, K.D. Osborne, SAE Paper 2000-01-1061, 2000.
[25] D. McKay, A. Stefanopoulou, Proc. 2004 Am. Control Conf. (2004) 816–821.